THE ASTROPHYSICAL JOURNAL, 582:L75–L78, 2003 January 10

GRB 021004: REVERSE SHOCK EMISSION

SHIHO KOBAYASHI[1,2] AND BING ZHANG[2]

Received 2002 October 26; accepted 2002 December 2; published 2002 December 11

ABSTRACT

We show that the rebrightening in the GRB 021004 optical afterglow light curve can be explained within the framework of the standard fireball model. The optical light curve of the forward shock emission is expected to rise initially and to decay after the typical synchrotron frequency crosses the optical band. We show that such a rising phase emission was caught for GRB 021004, together with a reverse shock emission. With the standard values of parameters obtained in other afterglow observations, we can construct example cases in which theoretical estimates reasonably fit the broadband observations. Therefore, the early rebrightening might be a common feature in optical afterglows.

Subject headings: gamma rays: bursts — hydrodynamics — relativity — shock waves

1. INTRODUCTION

GRB 021004 triggered the *High Energy Transient Explorer 2* (*HETE-2*) on 2002 October 4 at 12:06:13 UT. The burst lasted $T \sim 100$ s (Shirasaki et al. 2002), and the 7–400 keV fluence was $\sim 3.2 \times 10^{-6}$ ergs cm^{-2} (Lamb et al. 2002). The prompt localization of GRB 021004 by *HETE-2* allowed the follow-up of the afterglow at a very early time. Fox (2002) detected an optical transient ~9 minutes after the trigger at the level of $R \sim 15.56$ mag. Torii, Kato, & Yamaoka (2002) observed the error box of the burst ~3.5 minutes after the trigger, yielding an upper limit around $R \sim 13.6$ mag at the position of the transient discovered by Fox (2002). The spectroscopic observations of the optical afterglow revealed an emission line interpreted as Lyα at $z = 2.328$ (Mirabal et al. 2002). Assuming $\Omega_0 = 0.3$, $\lambda_0 = 0.7$, and $h = 0.6$, the isotropic gamma-ray energy is $\sim 5.6 \times 10^{52}$ ergs.

The dense sampling of the afterglow light curve at an early time revealed the peculiarity, a major rebrightening around ~0.1 days after the trigger and a short timescale variability around ~1 days. The slope of the afterglow is $\sim t^{-0.7}$ for the earliest three observations (9–17 minutes after trigger) by Fox (2002), and after the luminosity increased around ~0.1 days, it decayed with $\sim t^{-1.05}$ as afterglows usually do. These temporal features might be modeled by refreshed shocks (Zhang & Mészáros 2002). Recently, Lazzati et al. (2002) interpreted the features as being due to enhancements in the ambient medium density. In this Letter, we show that the major rebrightening around ~0.1 days can be explained within the standard fireball model. We propose that the reverse shock emission dominated the optical band at early times, leading to the observed peculiarity.

2. THE MODEL

Let us consider a relativistic shell (fireball ejecta) with energy E, a Lorentz factor η, and a width Δ_0 expanding into the homogeneous interstellar medium (ISM) with a particle number density n. When the shell sweeps a large volume of the ISM, it is decelerated, and the kinetic energy is transferred to the ISM by shocks (e.g., Kobayashi, Piran, & Sari 1999). The shocked ISM forms a relativistic blast wave (forward shock) and emits the internal energy via a synchrotron process.

The emission from a reverse shock was also predicted (Mészáros & Rees 1997; Sari & Piran 1999b). When the reverse shock crosses the shell, the forward-shocked ISM and the reverse-shocked shell carry comparable amounts of energy. However, the typical temperature of the shocked shell is lower since the mass density of the shell is higher. Consequently, the typical frequency in the shocked shell is lower. A prompt optical emission from GRB 990123 (Akerlof et al. 1999) can be regarded as this emission (Sari & Piran 1999a; Kobayashi & Sari 2000; Soderberg & Ramirez-Ruiz 2002).

2.1. *Forward Shock*

Observations of optical afterglows usually start around several hours after the burst trigger. Since, at such a late time, the typical synchrotron frequency of the forward shock emission $\nu_{m,f}$ is lower than the optical band $\nu_R \sim 5 \times 10^{14}$ Hz, the evolution of afterglows is well described by a single power law, except for the jet break (Rhoads 1999; Sari, Piran, & Halpern 1999). However, an optical light curve is expected to peak at an early time when the typical synchrotron frequency crosses the optical band. Before the peak time $t_{m,f}$, the luminosity increases proportional to $t^{1/2}$, reaches the maximum flux $F_{\nu,\max,f}$, and then decays proportional to $t^{3(1-p)/4}$, where p is the index of the power-law distribution of random electrons accelerated at the shock. Using the results in Sari, Piran, & Narayan (1998), we get

$$\nu_{m,f}(t) \sim 5.1 \times 10^{15}(1+z)^{1/2}\epsilon_B^{1/2}\epsilon_e^2 g^2 E_{52}^{1/2} t_d^{-3/2} \text{ Hz}, \quad (1)$$

$$\nu_{c,f}(t) \sim 2.7 \times 10^{12}(1+z)^{-1/2}\epsilon_B^{-3/2} E_{52}^{-1/2} n_0^{-1} t_d^{-1/2} \text{ Hz}, \quad (2)$$

$$t_{m,f} \sim 2.9(1+z)^{1/3}\epsilon_B^{1/3}\epsilon_e^{4/3} g^{4/3} E_{52}^{1/3} \nu_{R,15}^{-2/3} \text{ days}, \quad (3)$$

$$F_{\nu,\max,f} \sim 1.1 \times 10^2 a_\nu (1+z)\epsilon_B^{1/2} E_{52} n_0^{1/2} D_{28}^{-2} \text{ mJy}, \quad (4)$$

where $\nu_{c,f}$ is the cooling frequency, ϵ_B and ϵ_e are the fractions of the shock energy given to the magnetic field and electrons at the shock, respectively, $g = (p-2)/(p-1)$, $E_{52} = E/10^{52}$ ergs, $n_0 = n/1$ proton cm^{-3}, $\nu_{R,15} = \nu_R/10^{15}$ Hz, t_d is the observer's time in units of days, D_{28} is the luminosity distance in units of 10^{28} cm, and a_ν is a correction factor to the extinction along the line of sight to the burst.

Assuming that the rebrightening with the peak luminosity of ~1 mJy around ~0.1 days is caused by this peak, we get

[1] Department of Physics, 104 Davey Laboratory, Pennsylvania State University, University Park, PA 16802.
[2] Department of Astronomy and Astrophysics, 525 Davey Laboratory, Pennsylvania State University, University Park, PA 16802.

the following formulae for ϵ_e and n_0 as functions of ϵ_B and other known parameters:

$$\epsilon_e \sim 9.4 \times 10^{-2}\epsilon_B^{-1/4}\left(\frac{1+z}{3.3}\right)^{-1/4}\left(\frac{g}{0.29}\right)^{-1}\left(\frac{t_{m,f}}{0.1\ \mathrm{days}}\right)^{3/4} \times \left(\frac{E_{52}}{5.6}\right)^{-1/4}\left(\frac{\nu_{R,15}}{0.5}\right)^{1/2}, \quad (5)$$

$$n_0 \sim 8.0 \times 10^{-4}\epsilon_B^{-1}\left(\frac{a_\nu}{0.8}\right)^{-2}\left(\frac{1+z}{3.3}\right)^{-2}\left(\frac{F_{\nu,\max,f}}{1\ \mathrm{mJy}}\right)^{2} \times \left(\frac{E_{52}}{5.6}\right)^{-2}\left(\frac{D_{28}}{6.8}\right)^{4}. \quad (6)$$

Holland et al. (2002d) claim the extinction $A_V = 0.26$ mag, which implies an ~20% correction in the R band. The ~ -1.05 slope of the optical afterglow at a late time implies $p \sim 2.4$. However, there is still some debate about the value of p (Sako & Harrison 2002; Holland et al. 2002d; Pandey et al. 2002). We will discuss two cases, $p = 2.2$ and 2.4.

2.2. *Reverse Shock*

The evolution of reverse shocks is classified into two cases (Kobayashi 2000). If the initial Lorentz factor of the shell η is larger than a critical value $\eta_c = (3E/32\pi nm_p c^2\Delta_0^3)^{1/8}$, where m_p is the mass of the proton, the reverse shock becomes relativistic in the frame of the unshocked shell material while crossing the shell and drastically decelerates the shell (thick-shell case). If $\eta < \eta_c$, the reverse shock cannot decelerate the shell effectively (thin-shell case). According to the internal shock model, the initial width of the shell Δ_0 is given by the intrinsic duration of the gamma-ray burst (GRB), $\sim cT/(1+z)$ (Kobayashi, Piran, & Sari 1997):

$$\eta_c \sim 190 n_0^{-1/8}\left(\frac{1+z}{3.3}\right)^{3/8}\left(\frac{T}{100\ \mathrm{s}}\right)^{-3/8}\left(\frac{E_{52}}{5.6}\right)^{1/8}. \quad (7)$$

The Lorentz factor at the shock crossing time is given by $\gamma_\times \sim \min[\eta, \eta_c]$. The shock crossing time is $t_\times \sim (\gamma_\times/\eta_c)^{-8/3}T$ (Sari & Piran 1999b; Kobayashi 2000).

Since at the shock crossing time, the forward- and reverse-shocked regions have the same Lorentz factor and internal energy density e, the cooling frequency of the reverse shock $\nu_{c,r}$ is equal to that of the forward shock $\nu_{c,f}$:

$$\nu_{c,r}(t_\times) \sim \nu_{c,f}(t_\times). \quad (8)$$

The typical frequency of synchrotron emission is proportional to the electron's random Lorentz factor squared and to the magnetic field and Lorentz boost. The Lorentz boost and the magnetic field proportional to $\sqrt{e}$ are the same for the two shocked regions, while the random Lorentz factor is proportional to $\bar{\gamma}_\times$ in the reverse-shocked region and to $\gamma_\times$ in the forward-shocked region, where $\bar{\gamma}_\times$ is the Lorentz factor of the shocked shell material in the frame of the unshocked shell material. Using the relation $\gamma_\times\bar{\gamma}_\times \sim \eta$, the reverse shock frequency at the crossing time (the peak time) is given by (Sari & Piran 1999b)

$$\nu_{m,r}(t_\times) \sim \frac{\eta^2}{\gamma_\times^4}\nu_{m,f}(t_\times). \quad (9)$$

The peak flux at the typical frequency is proportional to the number of electrons and to the magnetic field and the Lorentz boost. From the energy conservation, the mass of the shell is larger by a factor of $\gamma_\times^2/\eta$ at the crossing time than that of the ISM swept by the forward shock. Since the number of electrons is proportional to the mass, we get

$$F_{\nu,\max,r}(t_\times) \sim \frac{\gamma_\times^2}{\eta}F_{\nu,\max,f}. \quad (10)$$

Even though the hydrodynamic evolutions of "thin" and "thick" shells are very different, the time dependences of the emission are similar (Kobayashi & Sari 2000). If the optical band ν_R is below the typical synchrotron frequency $\nu_{m,r}$, the luminosity decays as $\sim t^{-0.5}$. If $\nu_R > \nu_{m,r}$, it decreases as $\sim t^{-2}$ (Kobayashi 2000).

First we assume that the optical band is below the typical frequency of the reverse shock emission at the shock crossing time $\nu_{m,r}(t_\times) > \nu_R \sim \nu_{m,f}(t_{m,f})$. Using $\nu_{m,f} \propto t^{-3/2}$ (Sari, Piran, & Narayan 1998) and equation (9), we get $\eta > (T/t_{m,f})^{3/4}\eta_c^2 \sim 0.03\eta_c^2 > 1000$ for the standard values of parameters assumed in equation (7). Then GRB 021004 should be a thick-shell case. However, in a thick-shell case, we can show that $F(t_{\mathrm{eo}})/F_{\nu,\max,f} < Tt_{m,f}^{3/4}/t_{\mathrm{eo}}^{7/4} \sim 0.6$, where $F(t_{\mathrm{eo}})$ is the optical flux from the reverse shock at the earliest observations by Fox (2002) at $t_{\mathrm{eo}} \sim 0.01$ days. This limit is inconsistent with the observations, and hence $\nu_{m,r}(t_\times) < \nu_R$.

If $\nu_{m,r}(t_\times) < \nu_R$, the reverse shock emission simply decreases as t^{-2}. Since the extrapolation of the light curve from the data points by Fox (2002) to the earlier time $T \sim 10^{-3}$ days with a power law of t^{-2} violates the upper limits by Torii et al. (2002; see Fig. 1), GRB 021004 should be a thin-shell case, in which the peak of the reverse shock emission is delayed; i.e., $t_\times > T$.

Using equations (5) and (6) with $p = 2.4$, $t_{m,f} \sim 0.06$ days, $F_{\nu,\max,f} \sim 1.3$ mJy (R band), $E = 5.6 \times 10^{52}$ ergs, and $z = 2.3$, we search for a set of parameters (ϵ_B, η) with which the theoretical estimates give a reasonable fit to all observations. With a normalized Lorentz factor $\kappa \equiv \eta/\eta_c$, we can show that the crossing time $t_\times \propto \kappa^{-8/3}$ and that the optical flux from the reverse shock at the crossing time $F(t_\times) = (\nu_R/\nu_{m,r})^{-(p-1)/2} \times F_{\nu,\max,r} \propto \kappa^p\epsilon_B^{(2-p)/8}$. Since the optical flux $F(t_\times)$ depends on ϵ_B being very weakly proportional to $\epsilon_B^{-1/20}$ ($p = 2.4$) and $\epsilon_B^{-1/40}$ ($p = 2.2$), ϵ_B is not well determined from the light curve, or, equivalently, we can explain the peculiar behavior of the light curve with a wide range of ϵ_B. When changing the value of κ, the position of the peak moves along a line of $F \propto t^{-3p/8}$ on the flux-time plane, and $\kappa \sim 0.55$ gives the best fit to the observations. When we fitted the observations at greater than 0.1 days with a flatter power law of $t^{3(1-p)/4} = t^{-0.9}$ ($p = 2.2$), we needed to choose a earlier peak time $t_{m,f}$. Assuming the same parameters with the $p = 2.4$ case, except that $t_{m,f} \sim 0.035$ days, the best fit is given by $\kappa \sim 0.65$.

Since ϵ_e and n are determined by equations (5) and (6), $\nu_{m,f}$ and $F_{\nu,\max,f}$ do not depend on ϵ_B. The value of ϵ_B is constrained only by the cooling break. The cooling frequency $\nu_{c,f} \propto t^{-1/2}$ crosses the optical band at

$$t \sim 0.79\epsilon_B^{-1}\left(\frac{1+z}{3.3}\right)^{3}\left(\frac{E_{52}}{5.6}\right)^{3}\left(\frac{a_\nu}{0.8}\right)^{4}\left(\frac{F_{\nu,\max,f}}{1.3\ \mathrm{mJy}}\right)^{-4} \times \left(\frac{\nu_{R,15}}{0.5}\right)^{-2}\left(\frac{D_{28}}{6.8}\right)^{-8}\ \mathrm{days}.$$

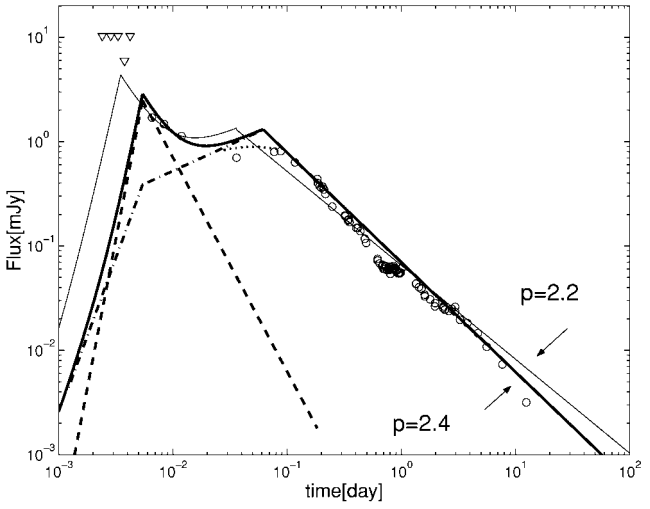

FIG. 1.—Optical light curve: Modeling with $p = 2.4$, forward shock emission (*dash-dotted line*), reverse shock emission (*dashed line*), total flux (*thick solid line*), and accurate spectrum mode (*dotted line*), $\epsilon_B = 3.0 \times 10^{-3}$, $\epsilon_e = 0.28$. $n = 0.45$ protons cm^{-3}, $\eta = 120$, and $E = 5.6 \times 10^{52}$ ergs. Modeling with $p = 2.2$ and total flux (*thin solid line*), $\epsilon_B = 3.0 \times 10^{-3}$, $\epsilon_e = 0.32$. $n = 0.45$ protons cm^{-3}, $\eta = 140$, and $E = 5.6 \times 10^{52}$ ergs. Measurements are shown as circles, and upper limits as triangles. Data are from Bersier et al. 2002b; Fox 2002; Halpern et al. 2002a, 2002b; Holland et al. 2002a, 2002b; Malesani et al. 2002a, 2002b; Masetti et al. 2002; Matsumoto et al. 2002a, 2002b; Mirabal et al. 2002a, 2002b; Oksanen & Aho 2002; Oksanen et al. 2002; Sahu et al. 2002; Stanek et al. 2002; Stefanon et al. 2002; Torii et al. 2002; Uemura et al. 2002; Weidinger et al. 2002; Winn et al. 2002; and Zharikov et al. 2002, following the calibration of Henden 2002.

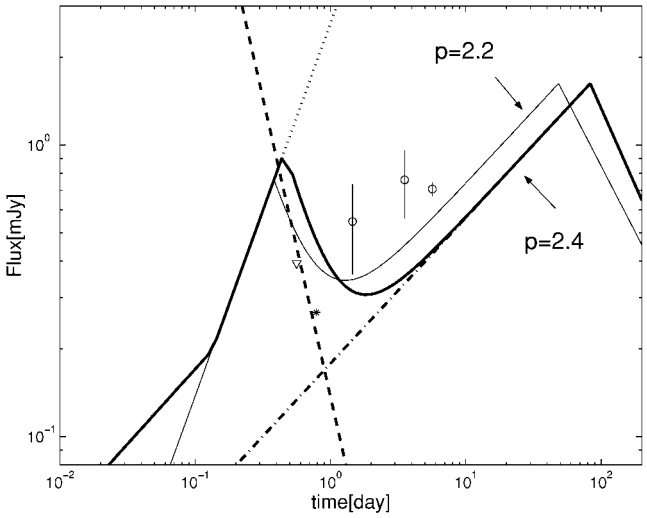

FIG. 2.—Radio light curve: Modeling with $p = 2.4$, forward shock emission (*dash-dotted line*), reverse shock emission (*dashed line*), self-absorption limit (*dotted line*), and total flux (*thick solid line*). Modeling with $p = 2.2$ and total flux (*thin solid line*). The parameters are the same as in Fig. 1. Measurements are shown as circles with error bars and as an asterisk, and the upper limit as a triangle. Data are from Frail & Berger 2002; Pooley 2002a, 2002b, 2002c; and Berger et al. 2002.

Holland et al. (2002d) report that there is no evidence for color evolution between 8.5 hr and 5.5 days after the burst (see, however, Matheson et al. 2002 and Bersier et al. 2002a) and hence that $\epsilon_B < 0.14$. A lower limit $\epsilon_B > 8 \times 10^{-5}$ is required from $\epsilon_e < 1$.

Figure 1 shows an example case in which $p = 2.4$ and $\epsilon_B = 3.0 \times 10^{-3}$ are assumed. This choice leads to $\epsilon_e \sim 0.28$, $n \sim 0.45$ protons cm^{-3}, and $\eta \sim 120$. These are surprisingly typical values obtained in other afterglow observations (Panaitescu & Kumar 2002). The dashed line and the dash-dotted line show the optical light curve of the reverse shock emission and the forward shock emission, respectively. The thick solid line depicts the total flux. Around the peak time of the forward shock (~0.1 days), our estimate slightly deviates from the observations. However, in our estimate, we assumed a simplified synchrotron spectrum that is described by a broken power law. Since a more realistic synchrotron spectrum is rounded at the break frequencies (Granot, Piran, & Sari 1999), a light curve should be also rounded at the break time (*dotted line*). The short timescale variability, which is prominent around ~1 day, might be produced by ISM turbulence (Wang & Loeb 2000; Holland et al. 2002c; Lazzati et al 2002). The latest data point in Figure 1 is lower than the extrapolation with a scaling of $t^{-1.05}$. This might be a signature of the jet break.

Assuming $p = 2.2$ and $\epsilon_B = 3.0 \times 10^{-3}$, we get $\epsilon_e \sim 0.32$, $n \sim 0.45$ protons cm^{-3}, and $\eta \sim 140$. The total flux is shown by the thin solid line. In this case, we need to assume larger ISM turbulence.

3. X-RAY AND RADIO AFTERGLOW

In this section, we assume the values of parameters with which we have shown the example cases in the previous section, and we estimate the X-ray and radio afterglows. The extinction correction a_ν is unity for X-ray and radio afterglows, and hence $F_{\nu,\max,f} \sim 1.6$ mJy (radio and X-ray).

X-ray afterglow.—Since the ~5 keV X-ray band is well above the typical frequency of the reverse shock emission, the contribution from the reverse shock to the X-ray band is negligible. The X-ray afterglow should be described only by the forward shock emission. The luminosity in the X-ray band should decrease as $t^{(2-3p)/4} \sim t^{-1.3}$ ($p = 2.4$) or $t^{-1.15}$ ($p = 2.2$). The *Chandra X-Ray Observatory* observed the afterglow for a total exposure of 87 ks, beginning October 5 8:55 UT (Sako & Harrison 2002). The count rate decreases with a power law slope of -1.0 ± 0.2. The mean 2–10 keV X-ray flux is $\sim 4.3 \times 10^{-13}$ ergs cm^{-2} s^{-1}. We estimate the 5 keV flux at the observational mean time of 1.36 days to be $\sim 3.1 \times 10^{-13}$ ergs cm^{-2} s^{-1} for $p = 2.4$ and $\sim 6.4 \times 10^{-13}$ ergs cm^{-2} s^{-1} for $p = 2.2$. Our estimates are in a good agreement with the observations.

Radio afterglow.—The forward shock emission in the ~10 GHz radio band increases as $t^{1/2}$ until the flux reaches the maximum of ~1.6 mJy at ~80 days for $p = 2.4$ (dash-dotted line in Fig. 2) or at ~50 days for $p = 2.2$. After the typical frequency $\nu_{m,r}$ crosses the radio band, the reverse shock emission decays as $\sim t^{-2}$ (dashed line for $p = 2.4$). At low frequencies and early times, self-absorption takes an important role and significantly reduces the flux. A simple estimate of the maximal flux (dotted line for $p = 2.4$) is the emission from the blackbody with the reverse shock temperature (Kobayashi & Sari 2000). The thick and thin solid lines depict the total flux for $p = 2.4$ and for $p = 2.2$, respectively. Since the observations (*circles*) are done in various frequencies, we scaled the observed value to the expected value at 10 GHz by using a spectral slope of 1.[3] This burst might also cause a bright radio flare ~1 mJy at around ~0.5 days, as observed in GRB 990123.

[3] Berger et al. (2002) reported an unusual spectral slope $F_\nu \sim \nu$ between 8.5 and 86 GHz from the observations with the Very Large Array on October 10.17 UT and claimed that the spectrum is not due to a transition from optically thick (ν^2) to optically thin ($\nu^{1/3}$) emission. The superposition of the forward and reverse shock emission could give an even flatter spectrum. A nonstandard emission mechanism may be needed to explain this unusual spectrum.

When we fitted the optical observations with $p = 2.2$, an earlier optical peak time $t_{m,f}$ is required. Since the peak time at the radio band is proportional to $t_{m,f}$, the modeling with $p = 2.2$ gives a better fit to the radio observations.

4. CONCLUSIONS

The low-frequency (e.g., optical, IR, and radio) light curve from the forward shock is expected to rise initially and to decay after the typical synchrotron frequency crosses the observational band. Although such a behavior has been observed in the radio band, previous optical afterglow observations were only made at too late times to catch the rising phase. However, the swift localization of GRB 021004 by *HETE-2* allowed the follow-up of the afterglow at a very early time. So far, this burst has the earliest detected optical afterglow. We have shown that the rising phase of the optical emission might be caught for the first time in GRB 021004, together with a reverse shock emission. The superposition of both the forward shock emission and the reverse shock emission can be well fitted for the 0.1 day rebrightening feature. With the standard values of parameters inferred from other afterglow observations, we have constructed example cases in which theoretical estimates fitted the broadband observations. We therefore suggest that the early rebrightening might be a common feature in optical afterglows.

The reverse shock emission in GRB 990123 peaked at about ~1 Jy in the *R* band, while the peak in GRB 021004 was only a few millijanskys. Since GRB 990123 is a very bright burst with a fluence about 100 times that of GRB 021004, we expect that GRB 990123 could produce the much brighter reverse shock emission. Another difference is the typical frequency $\nu_{m,r}(t_\times)$. In GRB 990123, it is close to the *R* band (Sari & Piran 1999a), while in GRB 021004, it is estimated as $\sim 1.4 \times 10^{12}$ Hz ($p = 2.4$) or $\sim 8.8 \times 10^{11}$ Hz ($p = 2.2$). The lower $\nu_{m,r}(t_\times)$ also makes the reverse shock emission dimmer in the *R* band (Kobayashi 2000).

We thank Peter Mészáros for his valuable comments and the anonymous referee for his/her valuable suggestions. We acknowledge support from the Center for Gravitational Wave Physics, which is funded by the NSF under cooperative agreement (PHY 01-14375), and from NASA (NAG5-9192).

REFERENCES

Akerlof, C. W., et al. 1999, Nature, 398, 400
Berger, E., et al. 2002, GCN 1613 (http://gcn.gsfc.nasa.gov/gcn/gcn3/1613.gcn3)
Bersier, D., et al. 2002a, ApJL, submitted (astro-ph/0211130)
Bersier, D., Winn, J., Stanek, K. Z., & Garnavich, P. 2002b, GCN 1586 (http://gcn.gsfc.nasa.gov/gcn/gcn3/1586.gcn3)
Fox, D. W. 2002, GCN 1564 (http://gcn.gsfc.nasa.gov/gcn/gcn3/1564.gcn3)
Frail, D., & Berger, E. 2002, GCN 1574 (http://gcn.gsfc.nasa.gov/gcn/gcn3/1574.gcn3)
Granot, J., Piran, T., & Sari, R. 1999, ApJ, 513, 679
Halpern, J. P., Armstrong, E. K., Espaillat, C. C., & Kemp, J. 2002a, GCN 1578 (http://gcn.gsfc.nasa.gov/gcn/gcn3/1578.gcn3)
Halpern, J. P., Mirabal, N., Armstrong, E. K., Espaillat, C. C., & Kemp, J. 2002b, GCN 1593 (http://gcn.gsfc.nasa.gov/gcn/gcn3/1593.gcn3)
Henden, A. 2002, GCN 1583 (http://gcn.gsfc.nasa.gov/gcn/gcn3/1583.gcn3)
Holland, S. T., Fynbo, J. P. U., Weidinger, M., Egholm, M. P., & Levan, A. 2002a, GCN 1585 (http://gcn.gsfc.nasa.gov/gcn/gcn3/1585.gcn3)
Holland, S. T., Fynbo, J. P. U., Weidinger, M., Egholm, M. P., Levan, A., & Pedersen, H. 2002b, GCN 1597 (http://gcn.gsfc.nasa.gov/gcn/gcn3/1597.gcn3)
Holland, et al. 2002c, AJ, 124, 639
———. 2002d, AJ, submitted (astro-ph/0211094)
Kobayashi, S. 2000, ApJ, 545, 807
Kobayashi, S., Piran, T., & Sari, R. 1997, ApJ, 490, 92
———. 1999, ApJ, 513, 669
Kobayashi, S., & Sari, R. 2000, ApJ, 542, 819
Lamb, D., et al. 2002, GCN 1600 (http://gcn.gsfc.nasa.gov/gcn/gcn3/1600.gcn3)
Lazzati, D., Rossi, E., Covino, S., Ghisellini, G., & Malesani, D. 2002, A&A, in press (astro-ph/0210333)
Malesani, D., et al. 2002a, GCN 1607 (http://gcn.gsfc.nasa.gov/gcn/gcn3/1607.gcn3)
———. 2002b, GCN 1645 (http://gcn.gsfc.nasa.gov/gcn/gcn3/1645.gcn3)
Masetti, N., et al. 2002, GCN 1603 (http://gcn.gsfc.nasa.gov/gcn/gcn3/1603.gcn3)
Matheson, T., et al. 2002, ApJL, submitted (astro-ph/0210403)
Matsumoto, K., Kawabata, T., Ayani, K., Urata, Y., & Yamaoka, H. 2002a, GCN 1567 (http://gcn.gsfc.nasa.gov/gcn/gcn3/1567.gcn3)
Matsumoto, K., Kawabata, T., Ayani, K., Urata, Y., Yamaoka, H., & Kawai, N. 2002b, GCN 1594 (http://gcn.gsfc.nasa.gov/gcn/gcn3/1594.gcn3)
Mészáros, P., & Rees, M. J. 1997, ApJ, 476, 232
Mirabal, J., Armstrong, E. K., Halpern, J. P., & Kemp, J. 2002a, GCN 1602 (http://gcn.gsfc.nasa.gov/gcn/gcn3/1602.gcn3)
Mirabal, J., Halpern, J. P., Chornock, R., &Filippenko, A. V. 2002b, GCN 1618 (http://gcn.gsfc.nasa.gov/gcn/gcn3/1618.gcn3)
Oksanen, A., & Aho, M. 2002, GCN 1570 (http://gcn.gsfc.nasa.gov/gcn/gcn3/1570.gcn3)
Oksanen, A., Aho, M., Rivich, K., Rivich, K.,West, D., & During, D. 2002, GCN 1591 (http://gcn.gsfc.nasa.gov/gcn/gcn3/1591.gcn3)
Panaitescu, A., & Kumar, P. 2002, ApJ, 571, 779
Pandey, S. B., et al. 2002, Bull. Astron. Soc. India, submitted (astro-ph/0211108)
Pooley, G. 2002a, GCN 1575 (http://gcn.gsfc.nasa.gov/gcn/gcn3/1575.gcn3)
———. 2002b, GCN 1588 (http://gcn.gsfc.nasa.gov/gcn/gcn3/1588.gcn3)
———. 2002c, GCN 1604 (http://gcn.gsfc.nasa.gov/gcn/gcn3/1604.gcn3)
Rhoads, J. E. 1999, ApJ, 525, 737
Sahu, D. K., Bhatt, B. C., Anupama, G. C., & Prabhu, T. P. 2002, GCN 1587 (http://gcn.gsfc.nasa.gov/gcn/gcn3/1587.gcn3)
Sako, M., & Harrison, F. A. 2002, GCN 1624 (http://gcn.gsfc.nasa.gov/gcn/gcn3/1624.gcn3)
Sari, R., & Piran, T. 1999a, ApJ, 517, L109
———. 1999b, ApJ, 520, 641
Sari, R., Piran, T., & Halpern, J. P. 1999, ApJ, 519, L17
Sari, R., Piran, T., & Narayan, R. 1998, ApJ, 497, L17
Shirasaki, Y., et al. 2002, GCN 1565 (http://gcn.gsfc.nasa.gov/gcn/gcn3/1565.gcn3)
Soderberg, A. M., & Ramirez-Ruiz, E. 2002, MNRAS, 330, L24
Stanek, K. Z., Bersier, D., Winn, J., & Garnavich, P. 2002, GCN 1598 (http://gcn.gsfc.nasa.gov/gcn/gcn3/1598.gcn3)
Stefanon, M., et al. 2002, GCN 1623 (http://gcn.gsfc.nasa.gov/gcn/gcn3/1623.gcn3)
Torii, K., Kato, T., & Yamaoka, H. 2002, GCN 1589 (http://gcn.gsfc.nasa.gov/gcn/gcn3/1589.gcn3)
Uemura, M., Ishioka, R., Kato, T., & Yamaoka, H. 2002, GCN 1566 (http://gcn.gsfc.nasa.gov/gcn/gcn3/1566.gcn3)
Wang, X., & Loeb, A. 2000, ApJ, 535, 788
Weidinger, M., et al. 2002, GCN 1573 (http://gcn.gsfc.nasa.gov/gcn/gcn3/1573.gcn3)
Winn, J., Bersier, D., Stanek, K. Z., Garvanich, P., & Walker, A. 2002, GCN 1576 (http://gcn.gsfc.nasa.gov/gcn/gcn3/1576.gcn3)
Zhang, B., & Mészáros, P. 2002, ApJ, 566, 712
Zharikov, S., Vazquez, R., Benitez, G., & del Rio, S. 2002, GCN 1577 (http://gcn.gsfc.nasa.gov/gcn/gcn3/1577.gcn3)